

# Structure and Properties of PP/POE/HDPE Blends

Yanhua Chen, Lin Ye

State Key Laboratory of Polymer Materials Engineering, Polymer Research Institute, Sichuan University, Chengdu 610065, China

Received 29 August 2010; accepted 5 November 2010

DOI 10.1002/app.33706

Published online 25 February 2011 in Wiley Online Library (wileyonlinelibrary.com).

**ABSTRACT:** This work was aimed to counteract the effect of ethylene- $\alpha$ -olefin copolymers (POE) by reinforcing the polypropylene (PP)/POE blends with high density polyethylene (HDPE) particles and, thus, achieved a balance between toughness and strength for the PP/POE/HDPE blends. The results showed that addition of HDPE resulted in an increasing wide stress plateau and more ductile fracture behavior. With the increase of HDPE content, the elongation at break of the blends increased rapidly without obvious decrease of yield strength and Young's modulus, and the notched izod impact strength of the blends can reach as high as 63 kJ/m<sup>2</sup> at 20 wt % HDPE loading. The storage modulus of PP blends increased and the glass transition temperature of each

component of the blends shifted close to each other when HDPE was added. The crystallization of HDPE phase led to an increase of the total crystallinity of the blend. With increasing HDPE content, the dispersed POE particle size was obviously decreased, and the interparticle distance was effectively reduced and the blend rearranged into much more and obvious core-shell structure. The fracture surface also changed from irregular striation to the regularly distant striations, displaying much obvious character of tough fracture. © 2011 Wiley Periodicals, Inc. *J Appl Polym Sci* 121: 1013–1022, 2011

**Key words:** polypropylene; high density polyethylene; blends; toughness; strength

## INTRODUCTION

PP is a widely produced, versatile, commodity polymer with a series of desirable properties, that is, low cost, easy processability combined with excellent mechanical and thermal properties. However, neat PP may exhibit high notch sensitivity and poor fractured toughness especially at low temperature, which limits its wide applications. In recent years, multiple elastomers have been added in PP to improve its toughness, such as ethylene-propylene random copolymer (EPR),<sup>1</sup> ethylene-propylene-diene terpolymer (EPDM),<sup>2</sup> and styrene-ethylene/butylene-styrene triblock copolymer (SEBS),<sup>3</sup> whereas the ethylene- $\alpha$ -olefin copolymers (POE) were proved to be more efficient in improving the toughness of PP due to the low interfacial tension between the two components.<sup>4</sup> Unfortunately, the soft modifier may cause a noticeable reduction in strength and modulus of blends, which cannot be completely solved by further addition of inorganic fillers, although it is supposed to increase the modulus of PP.<sup>5</sup> A delicate balance among modulus, yield/brittle stress, yield/brittle strain, and toughness has to be reached to achieve the system with all improved toughness, strength,

and modulus. Consequently, based on the concept "rigid-rigid polymer toughening,"<sup>6</sup> it is possible to improve both modulus and toughness of PP by blending with a rigid polymer.

Bai et al.<sup>7</sup> investigated on the blends of PP/polyamide6 (PA6)/POE. It was found that the toughness of the PP/PA6/POE blends increased with the content of alloying (PA6 + POE) without obvious decrease of Young's modulus or yield stress. Wei et al.<sup>8</sup> studied on the morphology and mechanical behavior of isotactic polypropylene (iPP)/Noryl [polyphenylene oxide (PPO) + high impact polystyrene (HIPS)] blends. The results showed that the fracture toughness of iPP could be significantly improved by adding rigid Noryl without causing any reduction in modulus. Additionally, the addition of a small amount of styrene-ethylene-propylene (SEP) compatibilizer greatly reduced Noryl particle size and improved particle-matrix interfacial bonding, which further improved the fracture toughness of iPP. Dai et al.<sup>9</sup> proposed that styrene-ethylene-propylene-styrene (SEPS) displayed a remarkable compatibilizing effect in PP/polycarbonate (PC)/POE blends, thus the blends showed remarkably improved mechanical properties with balanced toughness and rigidity.

Recently, high density polyethylene (HDPE) with high molecular weight and crystallinity has attracted the attention of technologist on account of these advantages, that is, high impact resistance even at

Correspondence to: L. Ye (yelinwh@126.com).

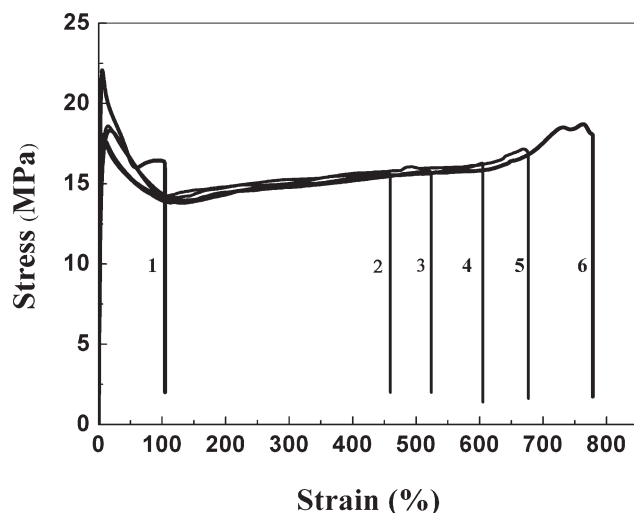


**Figure 1** Tensile stress–strain curves of PP blends: (1) PP/POE/HDPE (100/0/0); (2) PP/POE/HDPE (85/15/0); (3) PP/POE/HDPE (80/15/5); (4) PP/POE/HDPE (75/15/10); (5) PP/POE/HDPE (70/15/15); (6) PP/POE/HDPE (65/15/20).

low temperatures, good stiffness, strength, and thermal resistance.<sup>10</sup> PP and HDPE have, in many aspects, complementary properties, thus much research about the morphology,<sup>11</sup> mechanical properties,<sup>12</sup> and crystallization behavior<sup>13</sup> of PP/HDPE blends have been devoted to obtaining materials with good performance. In addition, scientists studied the effect of various types of compatibilizer: EPDM, SEBS, ethylene vinyl acetate and so forth in PP/HDPE blends.<sup>14–16</sup>

This work aimed to counteract the effect of POE by selectively reinforcing the PP/POE blends with HDPE particles, thus achieved a balance between toughness and strength for the PP/POE/HDPE blends. No works so far have been published on the system of PP/POE/HDPE blends. The influence of HDPE on morphology, crystallinity, and mechanical properties of PP/POE was investigated.

## EXPERIMENTAL

### Materials

PP SP179 (MFI = 10 g/10 min at 230°C) with 12.45 mol % ethylene was supplied by Lanzhou Petrochemical (Gansu, China). POE Engage 8150 (MFI = 0.5 g/10 min at 230°C) with 39 wt % octane was purchased from Dupont Dow Chemicals (Washington, USA). HDPE 5000S (MFI = 0.8–1.2 g/10 min at 190°C) was produced by Lanzhou Petrochemical (Gansu, China).

### Sample preparation

PP-based blends with 15 wt % POE and varying content of HDPE were prepared in a TSSJ-25/03,

corotating, twin-screw extruder at a rotational speed of 90 rpm. The temperature of the barrel was in the range of 170–220°C. Corresponding extrudates were hauled into a quenching water trough before being palletized. Dried blends were molded to form impact and tensile specimens by using a K-TEC40 injection molding machine. The barrel temperature profile was 180–230°C, and the mold temperature was maintained at 50°C.

## Measurements

### Mechanical property

The tensile properties and Young's modulus of PP blends were measured with 4302 material testing machine from Instron (USA) according to ISO527/1-1993 (E). The test speed was 50 and 2 mm/min for tensile properties and Young's modulus, respectively. The sample length between bench marks was 50 ± 0.5 mm.

The notched izod impact strength of PP blends was measured with XJU-5.5 impact testing machine from Jinjian (Chengde of China) according to ISO180-2001.

### Dynamic mechanical analysis

The dynamic mechanical analysis (DMA) of PP blends was performed with DMA Q800 (USA) by using three-point bending mode with a frequency of 1 Hz. The temperature scan ranged from –130 to 165°C with a heating rate of 5°C/min.

### Differential scanning calorimetry

The nonisothermal crystallization of PP blends was performed with a NETZSCH DSC 204 (Germany). Samples of 5–10 mg in weight were heated quickly from ambient temperature to 200°C in a nitrogen atmosphere and kept for 5 min before crystallization to eliminate the effect of the previous thermal history. The samples were then cooled down to 30°C at a cooling rate of 10°C/min and heated to 200°C at the same rate for data collection.  $X_c$  can be calculated with the following equation:

$$X_c = \frac{\Delta H_{mHDPE}}{\chi_{HDPE} \Delta H_{0HDPE}} \times 100\%$$

$$X_c = \frac{\Delta H_{mPP}}{\chi_{PP} \Delta H_{0PP}} \times 100\% \quad (1)$$

Where  $\Delta H_{mHDPE}$  and  $\Delta H_{mPP}$  are the measured melting enthalpy of HDPE and PP phases, respectively.  $\Delta H_{0HDPE}$  and  $\Delta H_{0PP}$  are the melting enthalpy of perfectly crystalline HDPE ( $\Delta H_{0HDPE} = 289$  J/g) and PP

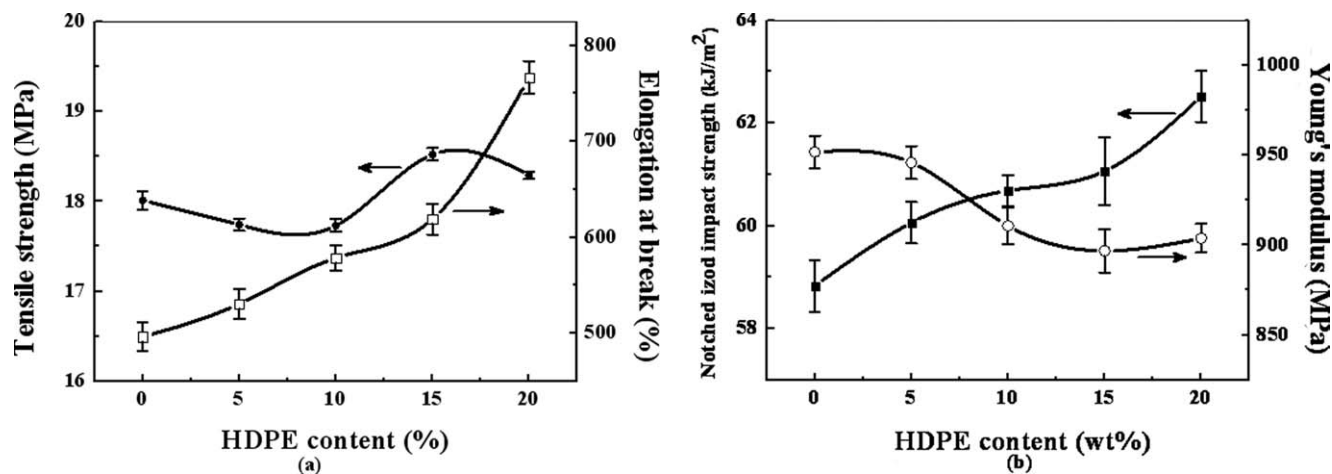


Figure 2 Tensile properties of PP blends as a function of HDPE content.

( $\Delta H_{0PP} = 209$  J/g), respectively.  $\chi_{HDPE}$  and  $\chi_{PP}$  are the blend composition, weight fraction of HDPE and PP phase, respectively.

#### Wide-angle X-ray diffraction

A wide-angle X-ray diffraction (WAXD) measurement was carried out with a Philip X'Pert Graphic & Identify instrument (The Netherlands) at room temperature to determine crystal parameters of PP blends. The Cu K $\alpha$  irradiation source was operated with a step size of  $0.02^\circ$  from  $2\theta = 10^\circ$ – $40^\circ$ , and the scanning rate was  $3^\circ/\text{min}$ . The d-spacing was calculated by substituting the scattering angles of the peak into the Bragg's equation<sup>17</sup> as follows:

$$d = \frac{\lambda}{2 \sin \theta} \quad (2)$$

Where  $\theta$  is X-ray diffraction angle and wavelength  $\lambda = 0.153$  nm.

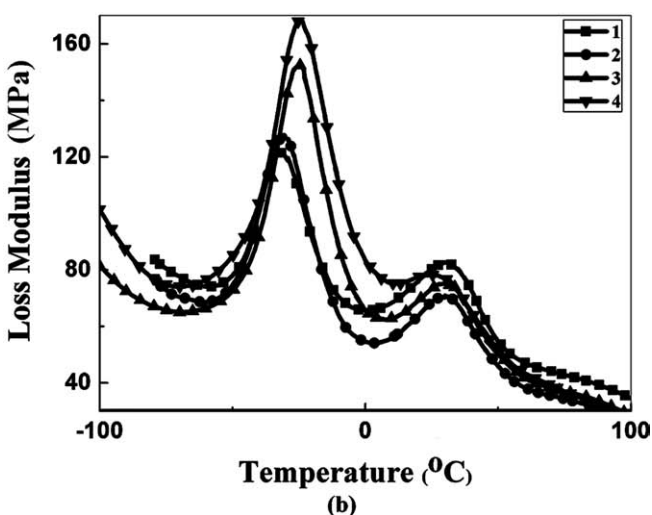
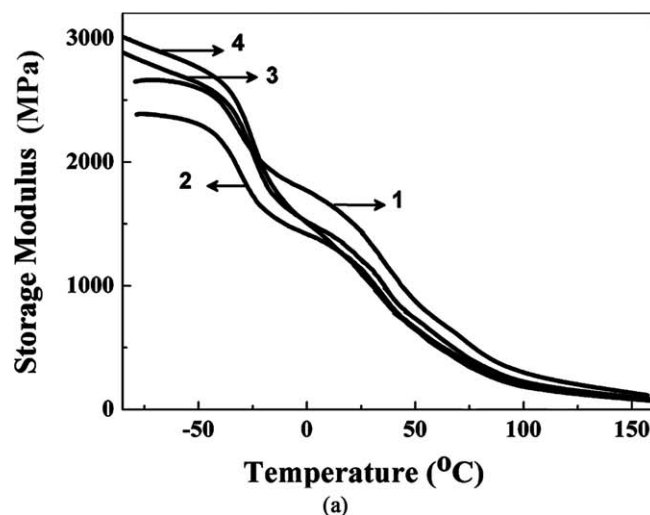


Figure 3 The storage modulus ( $E'$ ) and loss modulus ( $E''$ ) of PP blends: (1) PP/POE/HDPE (100/0/0); (2) PP/POE/HDPE (85/15/0); (3) PP/POE/HDPE (80/15/5); (4) PP/POE/HDPE (70/15/15).

#### Scanning electron microscopy analysis

Cryogenically fractured in liquid nitrogen and etched with dimethylbenzene to dissolve the POE and EPR phase at  $40^\circ\text{C}$  for 2.5 h, the fracture surfaces of PP blends were sputter-coated with a thin gold layer to make samples electric conductive, avoiding the charge accumulated, and then observed by a JEOL SM-5900LV scanning electron microscopy (SEM) instrument with an acceleration voltage of 20 kV. To study the toughening mechanism, the impact-fractured surface of the blends was directly observed under the same condition without etching.

## RESULTS AND DISCUSSION

### Effect of HDPE on the mechanical properties of PP/POE blends

In general, the mechanical properties of polymer can be roughly classified into two categories:

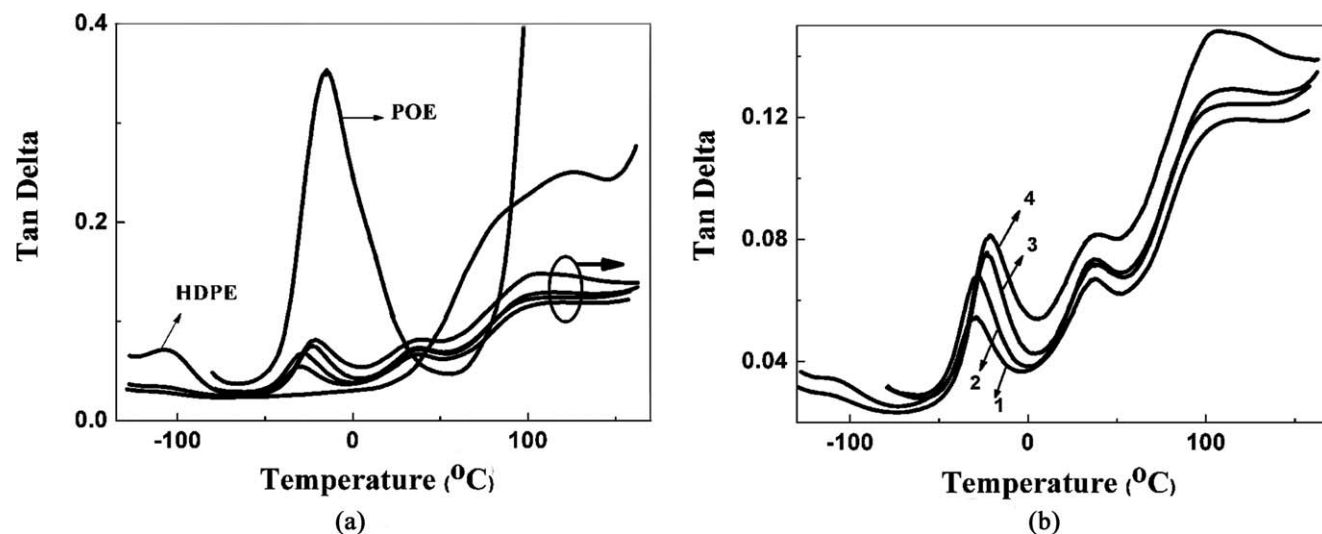


**Figure 4** The loss factor ( $\tan \delta$ ) of PP blends: (1) PP/POE/HDPE (100/0/0); (2) PP/POE/HDPE (85/15/0); (3) PP/POE/HDPE (80/15/5); (4) PP/POE/HDPE (70/15/15).

strength and toughness. Tensile strength and Young's modulus can be considered as the material strength, whereas tensile toughness and impact strength are the material toughness.<sup>18</sup> The tensile stress-strain curves of PP blends were shown in Figure 1. It can be seen that the stress-strain behavior of the blends varied dramatically with the composition of the blends. Neat PP showed the highest yield strength, and PP/POE blend exhibited elastic deformation stress plateau and typical ductile fracture. Addition of HDPE resulted in an increasing wide stress plateau and more ductile fracture behavior.

The mechanical properties of PP blends as a function of HDPE content were shown in Figure 2. It can be seen that with the increase of HDPE content, the elongation at break of the blends increased rapidly without obvious decrease of yield strength and Young's modulus. The notched izod impact strength of the blends was also significantly improved by addition of HDPE, which can reach as high as 63 kJ/m<sup>2</sup> at 20 wt % HDPE loading. Therefore, incorporation of HDPE into PP/POE blends can improve the toughness of the blends without deterioration of the strength, and a balance between toughness and strength was achieved.

#### Effect of HDPE on the dynamic mechanical properties of PP/POE blends

DMA has been used to ascertain the viscoelastic performance of materials under stress at different temperatures. The storage modulus is related to the elastic response of the tested material, and loss factor is associated with the chain relaxation that takes place.<sup>19</sup> Figure 3 was composite plot of temperature dependence of the storage modulus ( $E'$ ), loss modulus ( $E''$ ) of the blends.

All the storage modulus and temperature curves, as shown in Figure 3(a), experienced a gradual decline in storage modulus with increase in temperature from  $-130$  to  $165^\circ\text{C}$ . The addition of POE led to a reduction in storage modulus obviously, whereas when HDPE was added, there led to an increase in the modulus. The loss modulus [Fig. 3(b)] and  $\tan \delta$  (Fig. 4 and Table I) revealed the corresponding transition temperatures and the width of transition zones more obviously. In PP/POE binary system, the glass transition of POE occurred in the range of  $-55.30$  to  $-1.42^\circ\text{C}$  with a peak at about  $-28.60^\circ\text{C}$ . There exists a  $\beta$  transition of PP in the range of  $7.88$  to  $55.23^\circ\text{C}$  with a peak at about  $38.62^\circ\text{C}$  and a  $\alpha$ -relaxation peak around  $98.3^\circ\text{C}$ . These well-separated transitions are indicative of immiscibility of the component polymers. The different observation in Figure 4(b) was the appearance of a new transition peak around  $-108^\circ\text{C}$  by addition of 5 wt % HDPE in PP/POE blends. The peak temperature of the new transition was close to that of neat HDPE ( $-108.43^\circ\text{C}$ ). However, the glass transition peak of POE was noted at around  $-26.59^\circ\text{C}$ , which was higher than that of PP/POE blends. When more HDPE was added, broader and stronger transition was noted in this region of POE component and the

**TABLE I**  
Glass Transition Temperature of PP Blends

Sample	$T_g/^\circ\text{C}$ (PP)	$T_g/^\circ\text{C}$ (POE)	$T_g/^\circ\text{C}$ (HDPE)
PP	38.62	–	–
POE	–	$-15.98$	–
HDPE	–	–	$-108.43$
PP/POE (85/15)	38.62	$-28.60$	–
PP/POE/HDPE (80/15/5)	37.51	$-26.59$	$-108.06$
PP/POE/HDPE (70/15/15)	37.94	$-23.26$	$-104.91$

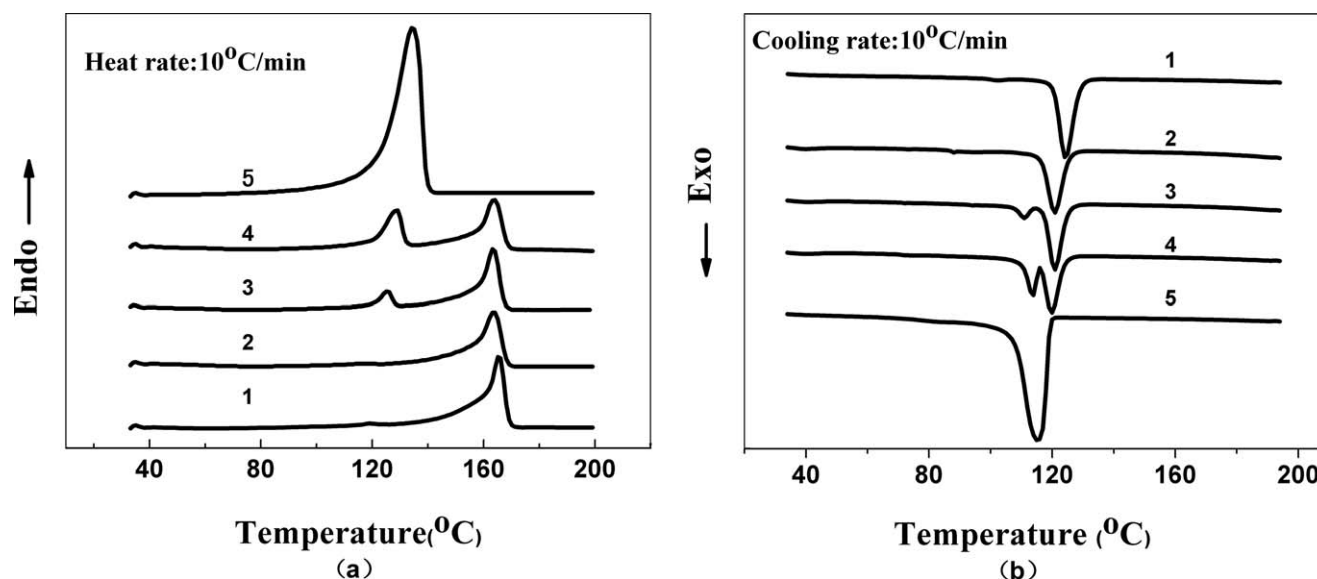


**Figure 5** DSC curves of PP blends: (1) PP/POE/HDPE (100/0/0); (2) PP/POE/HDPE (85/15/0); (3) PP/POE/HDPE (80/15/5); (4) PP/POE/HDPE (70/15/15); (5) PP/POE/HDPE (0/0/100).

transition shifted to higher temperature in the meantime, in other words, more close to the transition temperature of PP component.

Generally, glass transition shifts in the blends can be explained based on the physical interactions between the components. Compared with small molecules, it is more difficult for a macromolecule to mix with other components in the molecular level. But the data of DMA clearly showed that by addition of HDPE, each component of the blends exhibited a much more miscible with each other, and the interfacial tension tended to decrease and the compatibility of PP/POE/HDPE blend was improved.

#### Effect of HDPE on the crystallization behavior of PP/POE blends

The thermal behavior of different PP-based blends occurred during differential scanning calorimetry

(DSC) scan was shown in Figure 5, and the related data were listed in Table II. Both neat PP and neat HDPE were highly crystalline polymers with typical thermal behavior and exhibited a single crystallization and melting peak, respectively. Addition of POE made the melting and crystallization temperature of PP slightly decrease due to the fact that the amorphous component POE inserted into the crystalline lamellae and inhibited the crystallization process of PP, leading to the formation of small and imperfect PP crystal.

For PP/POE/HDPE blends, there appeared two crystallization and melting peaks, attributed to the crystallization of PP and HDPE, respectively. With increasing content of HDPE,  $T_c$  and  $T_m$  of PP phase exhibited basically unchangeable, whereas  $\Delta W_c$  and  $\Delta H_m$  of PP phase presented a decreasing tendency, indicating that the crystallization growth rate

**TABLE II**  
DSC Parameters for PP Blends

Sample	$T_{mOnset}^a$ (°C)		$T_m^b$ (°C)		$T_{cOnset}^c$ (°C)		$T_{cPeak}^d$ (°C)		$\Delta W^e$ (°C)		$\Delta H_m^f$ (J/g)		$X_c^g$ (%)	
	PP	HDPE	PP	HDPE	PP	HDPE	PP	HDPE	PP	HDPE	PP	HDPE	PP	HDPE
PP/POE/HDPE (100/0/0)	160.6	–	165.6	–	120.8	–	124.3	–	4.8	–	91.4	–	43.8	–
PP/POE/HDPE (85/15/0)	157.0	–	163.7	–	116.5	–	120.8	–	5.0	–	77.4	–	43.6	–
PP/POE/HDPE (80/15/5)	159.4	120.5	163.5	125.6	117.7	107.8	120.8	110.9	4.3	3.2	55.5	8.8	33.2	61.0
PP/POE/HDPE (70/15/15)	159.1	120.9	163.7	128.9	116.8	110.4	119.7	113.6	4.1	4.7	47.8	30.6	32.7	70.6
PP/POE/HDPE (0/0/100)	–	123.8	–	134.7	–	109.4	–	115.7	–	7.5	–	211.0	–	73.0

<sup>a</sup> The onset melting point.

<sup>b</sup> Melting point.

<sup>c</sup> The onset crystallization temperature.

<sup>d</sup> The crystallization peak temperature.

<sup>e</sup> The crystalline half-peak width.

<sup>f</sup> The melting enthalpy.

<sup>g</sup> The crystallinity.

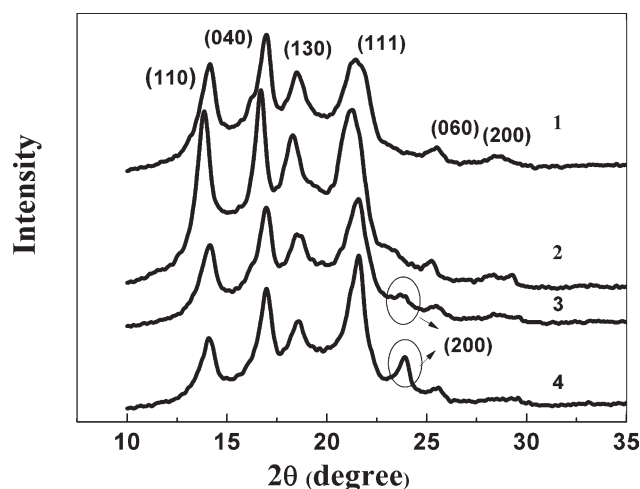


**Figure 6** WAXD patterns of PP blends: (1) PP/POE/HDPE (100/0/0); (2) PP/POE/HDPE (85/15/0); (3) PP/POE/HDPE (80/15/5); (4) PP/POE/HDPE (70/15/15).

increased, and the crystallinity of PP phase decreased. However, the crystallization of HDPE phase led to an increase of the total crystallinity of the blend.

The WAXD patterns of neat PP and the PP blends were given in Figure 6, and the related data were listed in Table III. The diffraction patterns of all the samples had a broad amorphous background. The neat PP showed four strong diffraction peaks at  $2\theta = 14.18^\circ$ ,  $17.09^\circ$ ,  $18.49^\circ$ , and  $21.19^\circ$ , corresponding to [110], [040], [130], and [111] lattice planes of  $\alpha$ -PP,<sup>20</sup> respectively. The PP/POE blend showed the same diffraction peaks as neat PP, and crystallization of PP was depressed. By addition of HDPE, the intensity of the characteristic peaks of PP slightly decreased. A new peak at  $2\theta = 23.96^\circ$  corresponding to the characteristic diffraction peak [200] of the

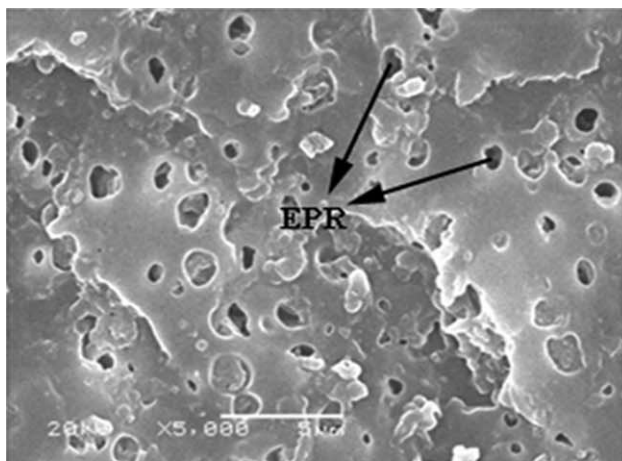
HDPE appeared, and the intensity of this diffraction peak increased with HDPE content. Moreover, the total crystallinity of the blend also increased with HDPE content, which was consistent with the DSC measurement. The results indicated that the increment of crystallinity of the blend with HDPE content made the strength and modulus maintained at a higher level.

#### Effect of HDPE on the morphology of PP/POE blends

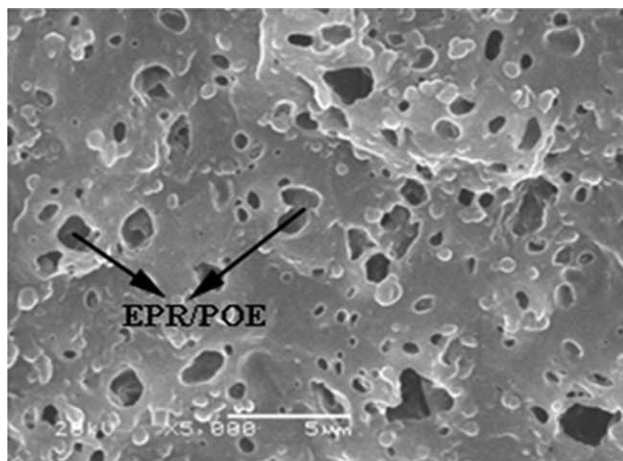
Figure 7 showed representative SEM micrographs of cryogenically fractured surface of PP blends with a typical matrix-dispersion structure. For neat PP, some dark holes can be observed, which came from the etched EPR elastomer phase. For PP/POE blend, much more amount of dark holes with increasing size representing the EPR and POE phase can be observed clearly. When the HDPE was added, three types of microstructures may form depending on the location of HDPE: "separate" dispersion structure, where the HDPE particles resided in the matrix and were not coated with POE/EPR elastomer; encapsulation or core-shell structure, where HDPE particles distributed preferentially in the dispersed elastomer phase; and mixture of the former two. With increasing HDPE content, the blend rearranged into much more and obvious core-shell structure [Fig. 7(d,e)]. The rheological property measurement showed that the melt viscosity of HDPE and POE were both higher than that of PP in the whole shear stress range, and the melt viscosity of HDPE was greater than that of POE in high shear stress range, whereas in low shear stress range, they were almost equal. Therefore, HDPE phase with higher viscosity formed

**TABLE III**  
WAXD Parameters of PP Blends

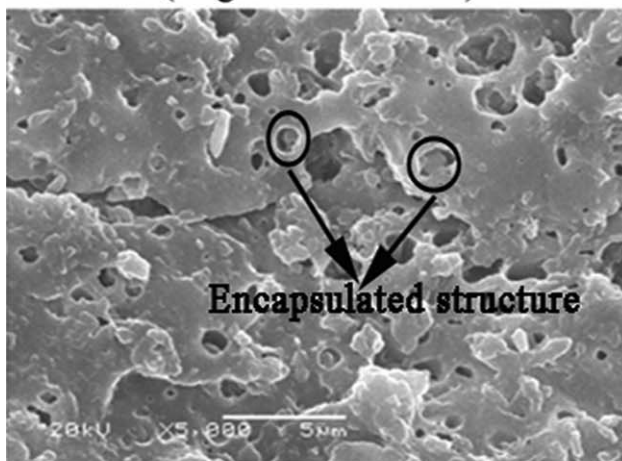
Samples	Diffraction peak	$2(\theta)$	$d$ (Å)	Relative intensity (%)	Total crystallinity (%)
PP/POE/HDPE (100/0/0)	110 ( $\alpha$ )	14.18	6.24	79.05	67.30
	040 ( $\alpha$ )	17.09	5.18	100.00	—
	130 ( $\alpha$ )	18.49	4.79	70.17	—
	111 ( $\alpha$ )	21.19	4.19	76.15	—
	041 ( $\alpha$ )	21.9	4.05	68.40	—
PP/POE/HDPE (85/15/0)	110 ( $\alpha$ )	13.99	6.32	99.96	59.55
	040 ( $\alpha$ )	16.74	5.29	90.12	—
	130 ( $\alpha$ )	18.27	4.85	100.00	—
	041 ( $\alpha$ )	21.68	4.09	52.25	—
	—	—	—	—	—
PP/POE/HDPE (80/15/5)	110 ( $\alpha$ )	13.96	6.33	66.13	69.79
	040 ( $\alpha$ )	16.68	5.30	100.00	—
	130 ( $\alpha$ )	18.32	4.83	62.80	—
	041 ( $\alpha$ )	21.30	4.17	95.67	—
	220	23.49	3.78	20.21	—
PP/POE/HDPE (70/15/15)	110 ( $\alpha$ )	14.04	6.30	42.08	73.50
	040 ( $\alpha$ )	16.97	5.22	79.72	—
	130 ( $\alpha$ )	18.69	4.74	54.77	—
	041 ( $\alpha$ )	21.65	4.10	100.00	—
	220	23.96	3.71	29.99	—



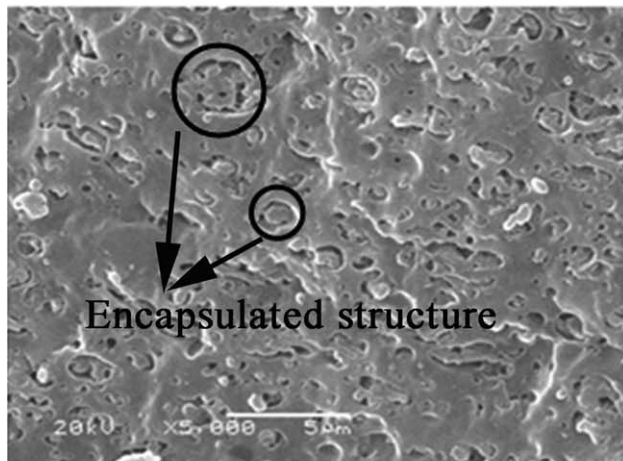
PP/POE/HDPE(100/0/0)  
(magnification:5000x)



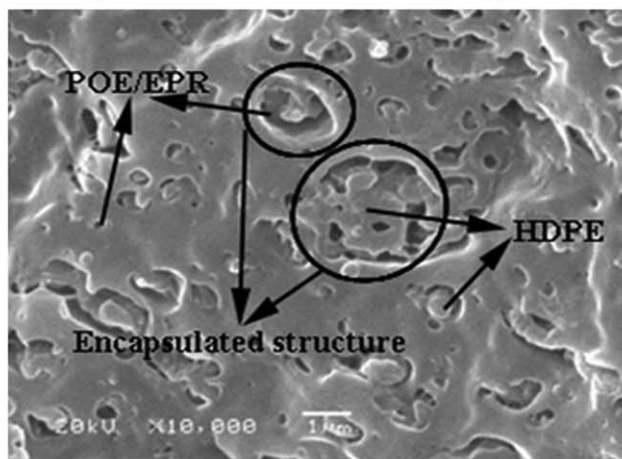
PP/POE/HDPE(85/15/0)  
(magnification:5000x)



PP/POE/HDPE(80/15/5)  
(magnification:5000x)



PP/POE/HDPE(70/15/15)  
(magnification:5000x)



PP/POE/HDPE(70/15/15)  
(magnification:10000x)

Figure 7 SEM images of etched PP blends.

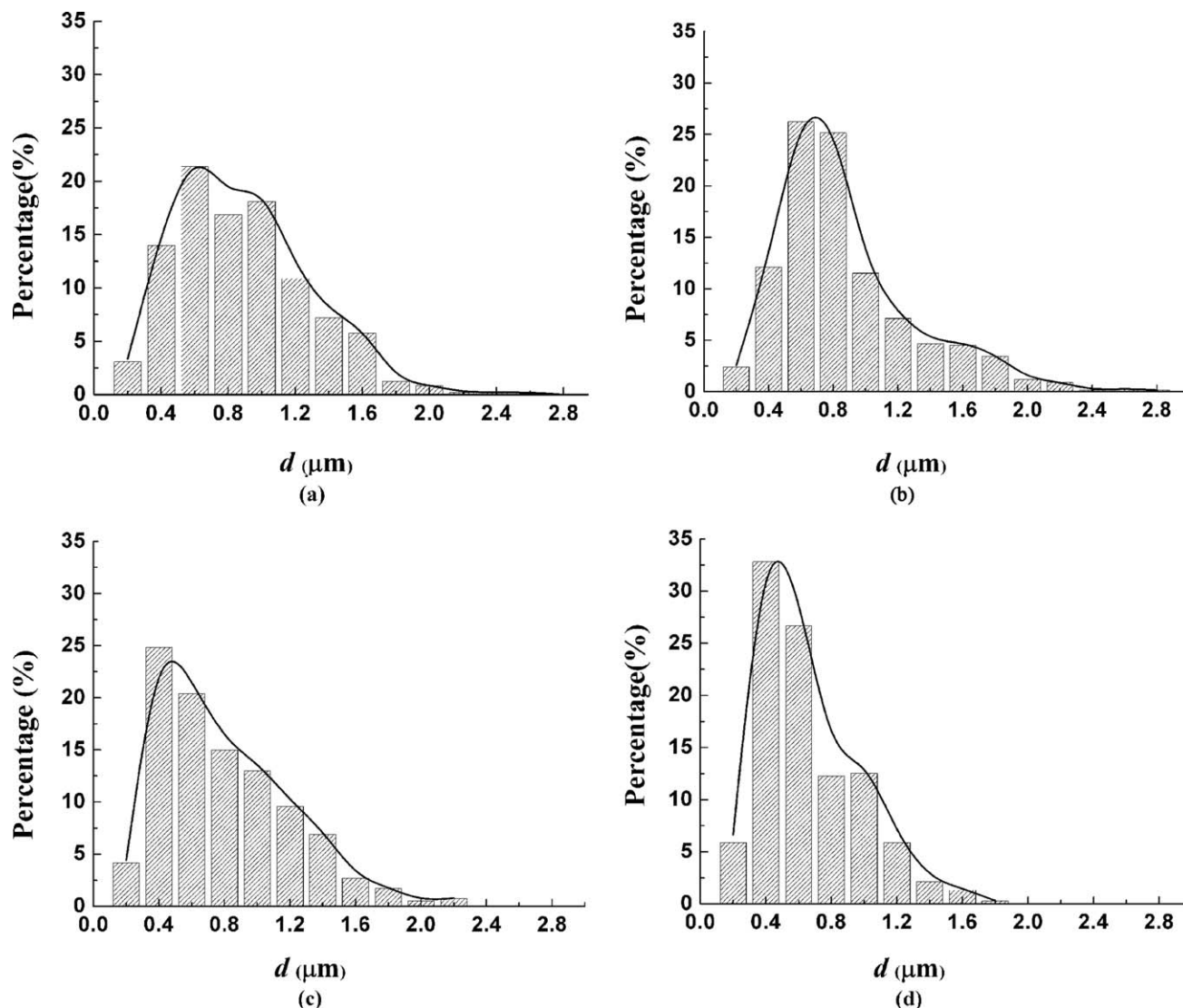


**Figure 8** Elastomer particle size distribution in PP blends: (a) PP/POE/HDPE (100/0/0); (b) PP/POE/HDPE (85/15/0); (c) PP/POE/HDPE (80/15/5); (d) PP/POE/HDPE (70/15/15).

the core and POE phase with lower viscosity formed the shell.<sup>21</sup>

#### Toughening mechanism of PP/POE/HDPE blends

Toughening mechanism in rubber-modified polymers has been well established.<sup>22,23</sup> According to the framework of Wu's theory,<sup>24,25</sup> for polymer/elastomer binary blend, a sharp brittle-ductile transition occurs at a critical matrix–ligament thickness or the critical surface-to-surface interparticle distance  $\tau_c$ , described by<sup>26</sup>:

$$\tau_c = d_c \left[ \left( \frac{\pi}{6\Phi_r} \right)^{1/3} - 1 \right] \quad (3)$$

where  $d_c$  is the critical elastomer particle diameter, and  $\Phi_r$  is the volume fraction of the elastomer. If  $\tau$  (average value)  $< \tau_c$ , the continuum percolation of stress volume around elastomer particles would occur. The matrix yielding would propagate through

the entire matrix, and then the blend would be tough. On the contrary, if  $\tau > \tau_c$ , the matrix yielding could not propagate, and the blend failed in a brittle manner. Following Wu's work, Li<sup>27</sup> extended the study and demonstrated that the critical matrix–ligament thickness of PP/Rubber blends was 0.15  $\mu\text{m}$ .

Further investigated on the PP/POE/HDPE blends, the matrix–ligament thickness can be calculated with the equation as follows, assuming that the POE/EPR elastomer particles are arranged in a cubic lattice.

$$\tau = d \left[ \left( \frac{\pi}{6\Phi_r} \right)^{1/3} - 1 \right] \quad (4)$$

where  $d$  is the diameter of elastomer particles, which can be obtained from SEM micrographs (Fig. 8);  $\Phi_r$  is volume fraction of elastomer particles, which can be calculated with the following equation.



**TABLE IV**  
Average Elastomer Particle Diameter and  $\tau$  Value of PP Blends

Sample	$\Phi_r$ (%)	$d$ ( $\mu\text{m}$ )	$\tau$ ( $\mu\text{m}$ )
PP/POE/HDPE (100/0/0)	22.7	0.772	0.248
PP/POE/HDPE (85/15/0)	34.6	0.778	0.115
PP/POE/HDPE (80/15/5)	34.6	0.705	0.104
PP/POE/HDPE (70/15/15)	34.6	0.560	0.083

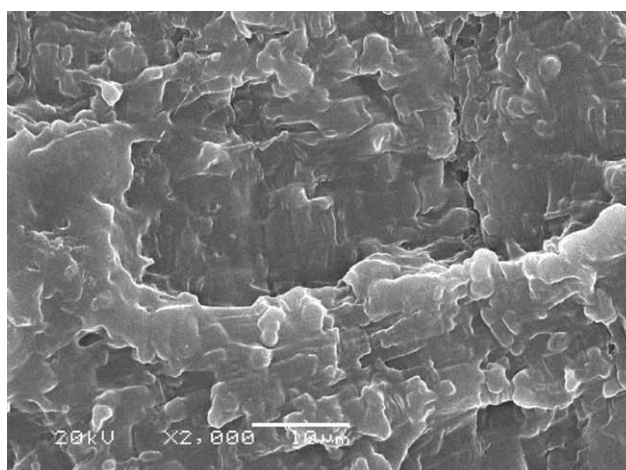
$$\phi_r = \frac{W_f \rho_m}{W_f \rho_m + (1 - W_f) \rho_f} \quad (5)$$

Where,  $W_f$ ,  $\rho_f$  are the mass fraction and density of elastomer particles, respectively;  $\rho_m$  is the density of PP matrix. The calculation results were listed in Table IV. It can be seen that the matrix–ligament thickness of neat PP was larger than the critical matrix–ligament thickness (0.15  $\mu\text{m}$ ), thus the neat PP exhibited the characteristics of brittle frac-

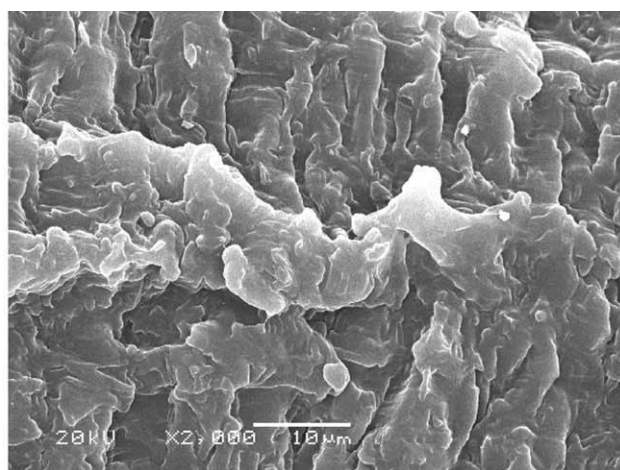
ture. For PP/POE blends, the matrix ligament thickness was lower than 0.15  $\mu\text{m}$ , and an obvious improvement of the impact strength (B–D transition) was observed. When the rigid HDPE was added, the dispersed POE particle size was obviously decreased, and the matrix ligament thickness was just 0.10  $\mu\text{m}$  or so, which resulted in earlier B–D transition onset. With increasing HDPE content, the matrix ligament thickness further decreased to 0.08  $\mu\text{m}$ . The results were consistent with the mechanical test.

Further insight into phase morphology of the blend, it can be seen that compared with PP blends in absence of HDPE, in PP/POE/HDPE blend, dispersed POE particle size was obviously decreased and the interparticle distance was effectively reduced, resulting in the increasing compatibility and toughness of the blends.

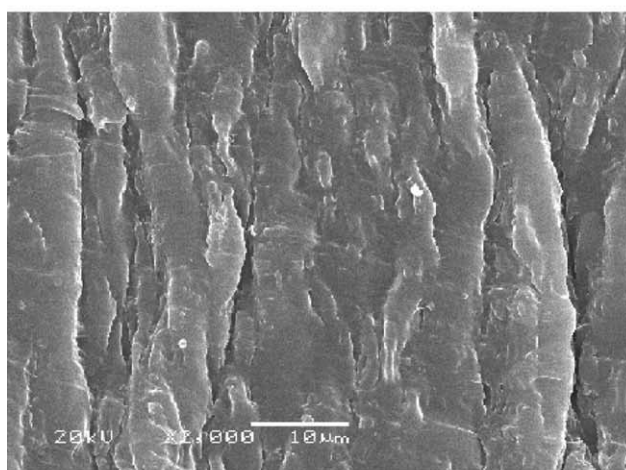
The impact-fracture surfaces of the blend were characterized via SEM, and the images were shown



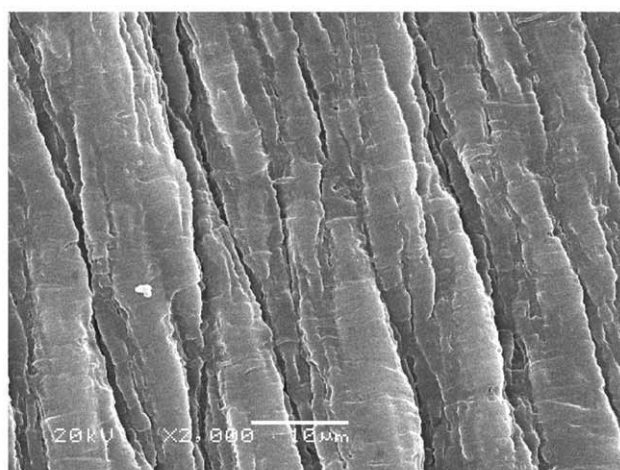
PP/POE/HDPE(100/0/0)



PP/POE/HDPE(85/15/0)



PP/POE/HDPE(80/15/5)



PP/POE/HDPE(70/15/15)

**Figure 9** SEM images of impact fracture surface of PP blends (magnification: 2000 $\times$ ).

in Figure 9. The fracture surface of neat PP was rough due to the slight toughening of EPR phase. By addition of POE, the blend exhibited increasing roughness. By further addition of HDPE, the fracture surface of the blend was fully covered with striations, indicating the severe plastic deformation. With increasing HDPE content, the fracture surface changed from irregular striation to regularly distant striations, displaying much obvious character of tough fracture.

Based on the above results, the great improvement of toughness in the PP/POE/HDPE blends was a result of synergistic effect of POE and HDPE. First, the elastomer particles can serve as stress concentrators to trigger and stabilize massive crazes in the PP matrix; second, the HDPE led to decrease of the dispersed POE particle size and interparticle distance. Thus, both crazing-shear banding mechanism and critical matrix ligament thickness mechanism can be used to explain the significantly improved toughness of PP/POE/HDPE blends. Moreover, the crystallinity of the blend also increased with HDPE content, and a balance between toughness and strength can be achieved.

### CONCLUSIONS

HDPE was utilized to significantly increase the toughness of PP/POE blends without sacrificing strength. The structure and properties of the blend were studied in terms of the mechanical properties, thermal properties, and morphologies. It was found that addition of HDPE resulted in an increasing wide stress plateau and more ductile fracture behavior. With the increase of HDPE content, the elongation at break of the blends increased rapidly without obvious decrease of yield strength and Young's modulus, and the notched izod impact strength of the blends was significantly improved, which can reach as high as 63 kJ/m<sup>2</sup> at 20 wt % HDPE loading. The storage modulus of PP blends increased when HDPE was added, and the glass transition temperature of each component of the blends shifted close to each other. For PP/POE/HDPE blends, there appeared two crystallization and melting peaks, attributed to the crystallization of PP and HDPE, respectively, and the crystallization of HDPE phase led to an increase of the total crystallinity of the blend. Three types of microstructures may form depending on the location of HDPE. With increasing HDPE content, the blend rearranged into much

more and obvious core-shell structure, whereas HDPE phase with higher viscosity formed the core, and POE phase with lower viscosity formed the shell. The dispersed POE particle size was obviously decreased, and the interparticle distance was effectively reduced with increasing HDPE content, resulting in an increasing compatibility and toughness of the blends. By addition of HDPE, the fracture surface changed from irregular striation to regularly distant striations, displaying much obvious character of tough fracture.

### References

1. Danesi, S.; Porter, R. S. *Polymer* 1978, 19, 448.
2. Van der Wal, A.; Mulder, J. J.; Oderkerk, J.; Gaymans, R. J. *Polymer* 1998, 39, 6781.
3. Gupta, A. K.; Purwar, S. N. *J Appl Polym Sci* 1984, 29, 1079.
4. McNally, T.; McShane, P.; Nally, G. M.; Murphy, W. R.; Cook, M.; Miller, A. *Polymer* 2002, 43, 3785.
5. Chang, S. Q.; Xie, T. X.; Yang, G. S. *J Appl Polym Sci* 2006, 102, 5184.
6. Wei, G. X.; Sue, H. J.; Chu, J.; Huang, C.; Gong, K. *J Mater Sci* 2000, 35, 555.
7. Bai, S. L.; Wang, G. T.; Hiver, J. M.; Christian, G. S. *Polymer* 2004, 45, 3063.
8. Wei, G. X.; Sue, H. J.; Chu, J.; Huang, C.; Gong, K. *Polymer* 2000, 41, 2947.
9. Dai, S. S.; Ye, L. *J Appl Polym Sci* 2008, 108, 3531.
10. Deanin, R. D.; Chung, C. H. *Handbook of Polyolefins-Synthesis and Properties*; Marcel Dekker: New York, 1993.
11. Souza, A. M. C.; Demarquette, N. R. *Polymer* 2002, 43, 3959.
12. Qian, X. Y.; Liu, F. H.; Song, Z. M.; Zhu, J.; Shen, K. Z.; Zhang, J. *Plast Sci Technol* 2009, 37, 29.
13. Zahran, R. R.; Konsowa, A. E. A. H.; EL-Latif, M. M. A.; Awwad, M. *J Appl Polym Sci* 2010, 115, 1407.
14. Vranjes, N.; Rek, V. *Macromol Symp* 2007, 258, 90.
15. Blom, H. P.; Teh, J. W.; Rudin, A. *J Appl Polym Sci* 1996, 60, 1405.
16. Souza, A. M. C.; Demarquette, N. R. *Polymer* 2002, 43, 3959.
17. Alexander, L. E. *X-ray Diffraction Methods in Polymer Science*; Wiley Interscience: New York, 1969.
18. Tseng, F. P.; Lin, J. J.; Tseng, C. R.; Chang, F. C. *Polymer* 2001, 42, 713.
19. Vivek, T.; Richard, L.; Thomas, N. *Polymer* 2006, 47, 5392.
20. Liu, Y. Q.; Kontopoulou, M. *Polymer* 2006, 47, 7731.
21. Santamaría, A.; Muñoz, M. E.; Peña, J. J.; Remiro, P. *Macromol Mater Eng* 1985, 134, 63.
22. Parker, D. S.; Sue, H. J.; Huang, J.; Yee, A. F. *Polymer* 1990, 31, 2267.
23. Kinloch, A. J.; Shaw, S. J.; Hunston, D. L. *Polymer* 1983, 24, 1341.
24. Margolina, A.; Wu, S. H. *Polymer* 1988, 29, 2170.
25. Wu, S. H. *J Appl Polym Sci* 1988, 35, 549.
26. Wu, S. H. *Polymer* 1985, 26, 1855.
27. Li, Q.; Zheng, W.; Qi, Z.; Zhu, X.; Choy, C. L. *Sci China Ser B* 1992, 22, 236.